

## Design of sodium carbonate functionalized TiO<sub>2</sub>-coated Fe<sub>3</sub>O<sub>4</sub> nanoparticles as a new heterogeneous catalyst for pyrrole synthesis

K. Fattahi, M. Farahi\*, B. Karami, R. Keshavarz

Department of Chemistry, Yasouj University, Yasouj 75918-74831, Iran

Received: July 07, 2020; Revised: December 03, 2021

The novel Fe<sub>3</sub>O<sub>4</sub>@TiO<sub>2</sub> supported sodium carbonate (Fe<sub>3</sub>O<sub>4</sub>@TiO<sub>2</sub>@(CH<sub>2</sub>)<sub>3</sub>OCO<sub>2</sub>Na) is reported with a view to introduce new synthetic routes under green and mild conditions. Additionally, it is shown this base-functionalized magnetic catalyst exhibits excellent activity for the synthesis of pyrroles *via* Paal-Knorr reaction. The structure of this catalyst was studied by FT-IR, XRD, SEM, EDS and VSM analysis. The separation of this catalyst is done in a facile manner by an external magnetic field and its use without reducing catalytic activity is possible for five times.

**Keywords:** pyrrole, Paal-Knorr reaction, nanocatalyst, Fe<sub>3</sub>O<sub>4</sub>, TiO<sub>2</sub>

### INTRODUCTION

Due to increasing environmental regulations, global safety of nature is the most important factor in modern science and technology, in particular, in the organic synthesis area. High activity and selectivity, and desired resilience of nanocatalysts make them to be recognized as pioneers of green chemistry. The important advantage of nanoparticles is their high specific surface area to volume ratio leading to increased contact with the reactants. Despite the several mentioned benefits of nanomaterials, they are difficult to separate. Therefore, it is important to design recoverable and green nanocatalysts [1, 2]. Heterogeneous catalysis using nanomaterials as recyclable catalysts for organic transformations has attracted the attention. Magnetic nanoparticles (MNPs) have been intensively investigated in recent years. Owing to the facility of isolation from the reaction mixture using an external magnet, as well as to the fact that such types of systems possess high-potential active sites for loading of other functional groups, it would be reasonable to use magnetic nanoparticles. Among them, nano-Fe<sub>3</sub>O<sub>4</sub> is most commonly used due to its unique physical properties including high surface area, superparamagnetism, low toxicity and their potential applications [3]. One of the inherent disadvantages of iron oxide nanoparticles is aggregation/oxidation and coating by metal oxides reduces this problem [4]. Titanium dioxide is a suitable substance for this purpose and can improve the catalytic activity of the magnetite nanoparticles. More attention is being paid to titania layer as coating of magnetic nanoparticles for increasing the surface area and simplifying the surface functionalization [5-7].

Pyrroles as an important class of heterocyclic compounds find widespread use in the pharmaceutical and agrochemical industries [8]. They are also widely applied in synthetic organic chemistry and material science. Pyrrole and its derivatives are also often seen as building blocks in naturally occurring and biologically active compounds. These heterocycles are prevalent in many drugs thus chemists are increasingly interested to discover new methods for rapid construction of pharmacologically important drug-like compounds [9]. So, it is not surprising that many synthetic approaches have been reported for the synthesis of pyrroles. The most widely used method is the Paal-Knorr synthesis, which consists of condensation of primary amines with 1,4-dicarbonyl compounds to obtain substituted pyrroles [10-12]. Numerous catalysts such as zeolite, Bi(NO<sub>3</sub>)<sub>3</sub>·5H<sub>2</sub>O, HCl, Ti(OPri)<sub>4</sub>, Al<sub>2</sub>O<sub>3</sub>, *p*-TSA, layered zirconium phosphate and zirconium sulfophenyl phosphonate have been applied in the Paal-Knorr reaction [13].

Synthesis of surface-modified magnetite nanoparticles is one of the major areas of our current research. In connection with our previous studies [14-20], we decided to introduce Fe<sub>3</sub>O<sub>4</sub>@TiO<sub>2</sub>@(CH<sub>2</sub>)<sub>3</sub>OCO<sub>2</sub>Na as a magnetically recoverable solid base catalyst.

### EXPERIMENTAL

All chemicals used in this research were purchased from Fluka and Merck chemical companies. Melting points were determined by an electrothermal KSB1N apparatus and are uncorrected. Fourier transform infrared (FT-IR) spectra were recorded on a Shimadzu-470 spectrometer using KBr pellets. X-ray powder diffraction (XRD) patterns were recorded using a

\* To whom all correspondence should be sent:

E-mail: farahimb@yu.ac.ir

Bruker AXS (D8 Advance) X-ray diffractometer with Cu K $\alpha$  radiation ( $\lambda = 0.15418$  nm). The measurement was made in  $2\theta$  ranging from 10° to 80° at the speed of 0.05° min<sup>-1</sup>. Energy dispersive spectroscopy (EDS) was performed using a TESCAN Vega model instrument. The morphology of the particles was observed by scanning electron microscopy (SEM) under an acceleration voltage of 26 kV. The magnetic measurement was carried out in a vibrating sample magnetometer (VSM) Kashan University, Kashan, Iran) at room temperature.

#### *Synthesis of Fe<sub>3</sub>O<sub>4</sub> MNPs*

FeCl<sub>3</sub>.6H<sub>2</sub>O (2.7 g, 10 mmol) and FeCl<sub>2</sub>.4H<sub>2</sub>O (1 g, 5 mmol) were dissolved in distilled water (45 mL) and stirred for 15 min under argon atmosphere at 80 °C. Sodium hydroxide solution (5 mL, 10 M) was then added dropwise to the solution as long as the color of solution was black. After about 1 h, the generated iron oxide nanoparticles were collected with a magnet and rinsed thoroughly with distilled water two or three times. MNPs Fe<sub>3</sub>O<sub>4</sub> was dried at 60 °C [21].

#### *Preparation of Fe<sub>3</sub>O<sub>4</sub>@TiO<sub>2</sub>*

Nano-Fe<sub>3</sub>O<sub>4</sub> was initially diluted in a mixture of ethanol and acetonitrile (125:45 mL). The resulting dispersion was then homogenized by ultrasonic vibration in a water bath. Then followed the addition of ammonia aqueous solution (0.75 mL, 25%) while stirred vigorously by a mechanical stirrer at room temperature for 30 min. Tetraethyl orthotitanate (TEOT) (1.5 mL) in absolute ethanol (20 mL) was then added dropwise to the solution under continuous mechanical stirring at 30 °C for 2 h. Fe<sub>3</sub>O<sub>4</sub>@-TiO<sub>2</sub> was separated by a magnet, washed several times with ethanol, and dried at room-temperature [22].

#### *Procedure for the synthesis of Fe<sub>3</sub>O<sub>4</sub>@TiO<sub>2</sub>@(CH<sub>2</sub>)<sub>3</sub>Cl*

Fe<sub>3</sub>O<sub>4</sub>@TiO<sub>2</sub> (0.5 g) was ultrasonically dispersed in dry toluene (80 mL) for 15 min. Next, 3-chloropropyltriethoxysilan (0.121 g, 0.5 mmol) was added to the mixture and stirred with argon gas under reflux conditions for 12 h. Next, Fe<sub>3</sub>O<sub>4</sub>@TiO<sub>2</sub>@(CH<sub>2</sub>)<sub>3</sub>Cl was obtained by magnetic separation and washed with deionized water and ethanol [18].

#### *Synthesis of Fe<sub>3</sub>O<sub>4</sub>@TiO<sub>2</sub>@(CH<sub>2</sub>)<sub>3</sub>OCO<sub>2</sub>Na (1)*

In the final step, the prepared Fe<sub>3</sub>O<sub>4</sub>@TiO<sub>2</sub>@(CH<sub>2</sub>)<sub>3</sub>Cl (0.5 g) was dissolved in DMSO (50 mL) and ultrasonicated for 15 min. Then Na<sub>2</sub>CO<sub>3</sub> (1 g) was added and the reaction mixture was heated at 90 °C for 24 h. The final product was separated from the solution with a magnet and then washed several times with water and ethanol followed by drying at 60 °C under vacuum.

#### *General procedure for the synthesis of pyrrole derivatives (4)*

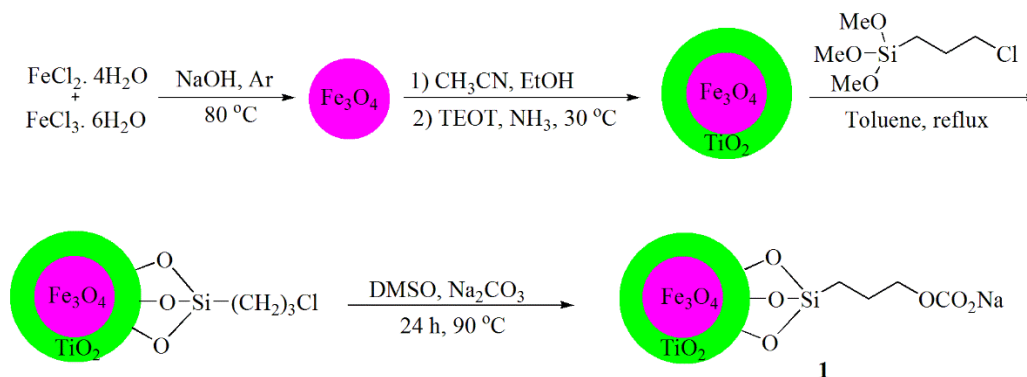
Fe<sub>3</sub>O<sub>4</sub>@TiO<sub>2</sub>@(CH<sub>2</sub>)<sub>3</sub>OCO<sub>2</sub>Na (0.003 g) was added to a mixture of 2,5-hexadione (1 mmol) and aniline derivatives (1 mmol) at 80 °C. The mixture was stirred under solvent-free conditions for 15-25 min and the reaction process was followed by thin-layer chromatography. After completion, the reaction mixture was dissolved in hot EtOH (5 mL). The catalyst was removed from the reaction mixture using an external magnet. The solvent was then removed and the crude products were purified by crystallization from *n*-hexane.

#### *Catalyst recovery instructions*

2,5-Hexadione (1 mmol), aniline (1 mmol), and Fe<sub>3</sub>O<sub>4</sub>@TiO<sub>2</sub>@(CH<sub>2</sub>)<sub>3</sub>OCO<sub>2</sub>Na (0.003 g) were stirred under free-solvent condition at 80 °C for 20 min. After completion of the reaction, hot ethanol (5 mL) was added to the reaction and the mixture was subjected to separation using a permanent magnet. It was repeatedly washed with distilled water (10 mL each), three times with methanol (10 mL each) and then dried at 80 °C. Finally, it was reused in subsequent runs.

## RESULTS AND DISCUSSION

The magnetic nanocatalyst Fe<sub>3</sub>O<sub>4</sub>@TiO<sub>2</sub>@(CH<sub>2</sub>)<sub>3</sub>OCO<sub>2</sub>Na (**1**) was prepared following the procedure shown in Scheme 1. Firstly, the chemical coprecipitation of Fe<sup>2+</sup> and Fe<sup>3+</sup> ions in basic solution led to the formation of nano-Fe<sub>3</sub>O<sub>4</sub>. Then, in order to avoid possible aggregation or oxidation of the iron oxide nanoparticles, the obtained MNPs were coated with TiO<sub>2</sub> using tetraethyl orthotitanate (TEOT). Nanoparticles Fe<sub>3</sub>O<sub>4</sub>@TiO<sub>2</sub> can be functionalized with 3-chloropropyltriethoxysilan molecule. Finally, the surface of Fe<sub>3</sub>O<sub>4</sub>@TiO<sub>2</sub>@(CH<sub>2</sub>)<sub>3</sub>Cl was functionalized with Na<sub>2</sub>CO<sub>3</sub> to give nanocatalyst **1**. The prepared catalyst was characterized by FT-IR, XRD, SEM, EDS and VSM analysis.



**Scheme 1.** Synthesis of Fe<sub>3</sub>O<sub>4</sub>@TiO<sub>2</sub>@(CH<sub>2</sub>)<sub>3</sub>OCO<sub>2</sub>Na (**1**).

Fig. 1 shows the XRD patterns of Fe<sub>3</sub>O<sub>4</sub>, Fe<sub>3</sub>O<sub>4</sub>@TiO<sub>2</sub> and Fe<sub>3</sub>O<sub>4</sub>@TiO<sub>2</sub>@(CH<sub>2</sub>)<sub>3</sub>OCO<sub>2</sub>Na. In Fig. 1c the peaks at  $2\theta = 30.2, 35.6, 43.4, 53.9, 57.4$  and  $63.0$  are related to (220), (311), (400), (422), (511) and (440) showing the cubic spinel structure of Fe<sub>3</sub>O<sub>4</sub> [23]. Also, the mentioned indices revealed that the new catalyst in Fig. 1c has a similar structure to Fe<sub>3</sub>O<sub>4</sub> nanoparticles in Fig. 1a, and this shows that no phase change was observed after surface modification of the magnetite nanoparticles. The characteristic peaks confirming the presence of -OCO<sub>2</sub>Na appeared around 10, 34, 36 and 43 ( $2\theta$ ), some of which were overlapped by Fe<sub>3</sub>O<sub>4</sub> peaks [24].

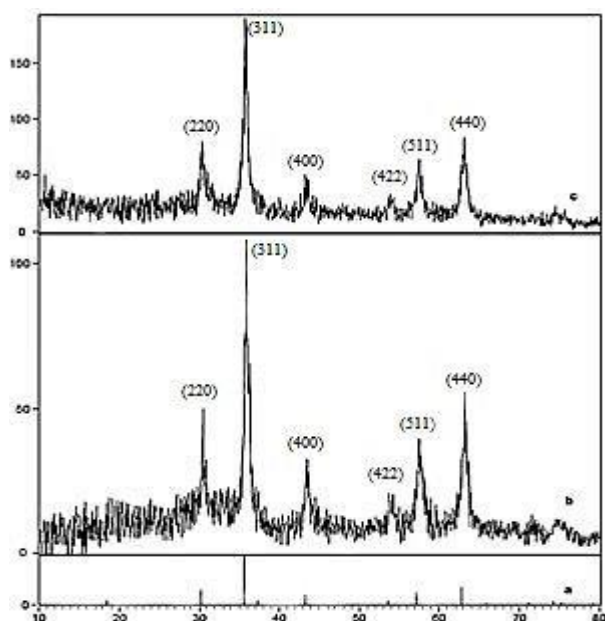


**Fig. 1.** XRD patterns of (a) Fe<sub>3</sub>O<sub>4</sub>, (b) Fe<sub>3</sub>O<sub>4</sub>@TiO<sub>2</sub>, and (c) Fe<sub>3</sub>O<sub>4</sub>@TiO<sub>2</sub>@(CH<sub>2</sub>)<sub>3</sub>OCO<sub>2</sub>Na.

The FT-IR spectra of Fe<sub>3</sub>O<sub>4</sub>, Fe<sub>3</sub>O<sub>4</sub>@TiO<sub>2</sub>, Fe<sub>3</sub>O<sub>4</sub>@-TiO<sub>2</sub>@(CH<sub>2</sub>)<sub>3</sub>Cl and Fe<sub>3</sub>O<sub>4</sub>@TiO<sub>2</sub>@(CH<sub>2</sub>)<sub>3</sub>OCO<sub>2</sub>Na were compared to analyze the progress of the designed catalyst (Fig. 2). The presence of characteristic peaks corresponding to Fe-O stretching vibration near 586 cm<sup>-1</sup> in all compared spectra is a confirmation of the

preservation of the nanostructure of Fe<sub>3</sub>O<sub>4</sub> throughout the process. The broad band between 400-700 and 1400 cm<sup>-1</sup> seen in Fig. 2b may be assigned to the Ti-O-Ti stretching modes and Fe-O-Ti bonds, respectively [25, 18]. In Fig. 2c, CH<sub>2</sub> bending, as a broad band and symmetric CH<sub>2</sub> and asymmetric CH<sub>2</sub> of the alkyl chains appeared at 1480 cm<sup>-1</sup> and 2860 to 2923 cm<sup>-1</sup> [23]. In Fig. 2d the peak related to -OCO<sub>2</sub>Na group appeared at 1407 and 1636 cm<sup>-1</sup> [24].

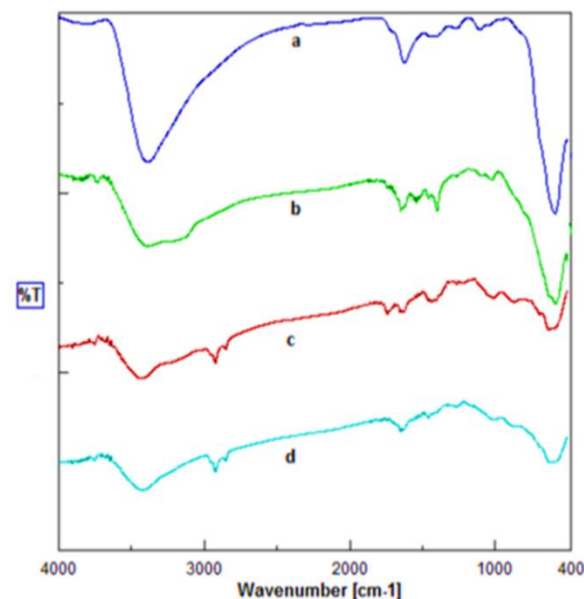


**Fig. 2.** The FT-IR spectra of (a) Fe<sub>3</sub>O<sub>4</sub> MNPs, (b) Fe<sub>3</sub>O<sub>4</sub>@TiO<sub>2</sub>, (c) Fe<sub>3</sub>O<sub>4</sub>@TiO<sub>2</sub>@(CH<sub>2</sub>)<sub>3</sub>Cl, and (d) Fe<sub>3</sub>O<sub>4</sub>@TiO<sub>2</sub>@(CH<sub>2</sub>)<sub>3</sub>OCO<sub>2</sub>Na.

The EDS pattern of the synthesized nanocatalyst **1** is shown in Fig. 3. It is seen that Fe<sub>3</sub>O<sub>4</sub>@TiO<sub>2</sub>@(CH<sub>2</sub>)<sub>3</sub>OCO<sub>2</sub>Na contains all expected elemental cases including Ti, O, Fe, C, Si and Na.

The SEM image of Fe<sub>3</sub>O<sub>4</sub>@TiO<sub>2</sub>@(CH<sub>2</sub>)<sub>3</sub>OCO<sub>2</sub>Na was recorded to show the morphology of the catalyst **1** (Fig. 4). This image shows the proper size of nanoparticles and their spherical shapes.

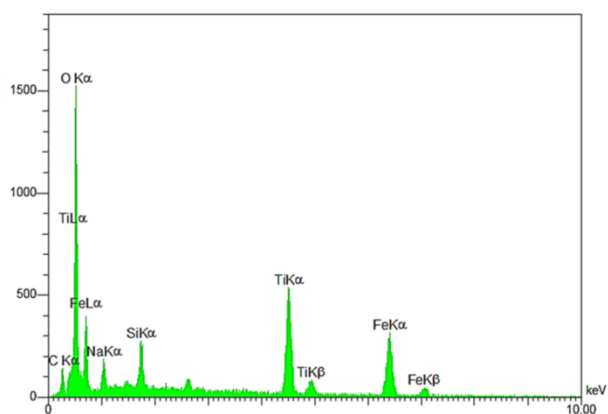


**Fig. 3.** EDS analysis of Fe<sub>3</sub>O<sub>4</sub>@TiO<sub>2</sub>@(CH<sub>2</sub>)<sub>3</sub>OCO<sub>2</sub>Na.

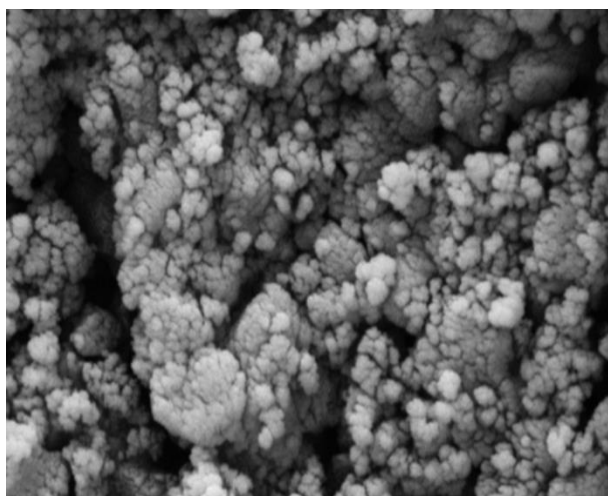


**Fig. 4.** SEM image of catalyst **1**.

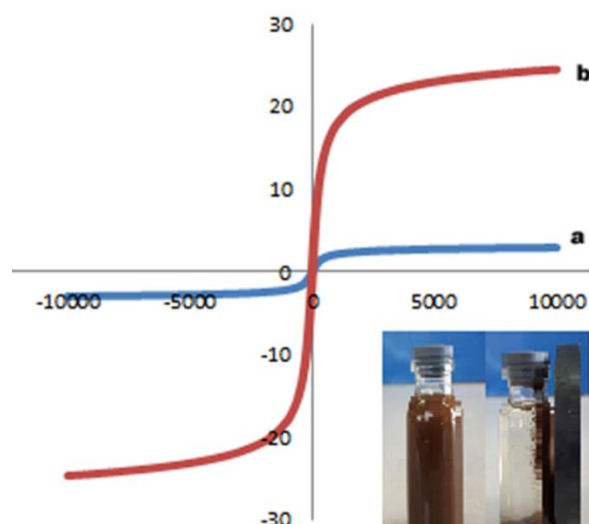
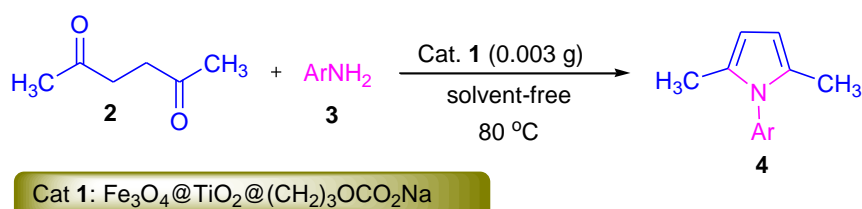


**Fig. 5.** Room-temperature magnetization curves of (a) Fe<sub>3</sub>O<sub>4</sub>@TiO<sub>2</sub>@(CH<sub>2</sub>)<sub>3</sub>OCO<sub>2</sub>Na and (b) recycled catalyst from the model reaction.

Fig. 5 shows the magnetization *versus* applied field of the catalyst obtained by VSM. Comparison of two curves is shown, which proves that the magnetic property is retained after the catalyst being used in the reaction.

Having successfully prepared the new nanocatalyst, we investigated the use of Fe<sub>3</sub>O<sub>4</sub>@TiO<sub>2</sub>@(CH<sub>2</sub>)<sub>3</sub>OCO<sub>2</sub>Na (**1**) as a novel reusable nanocatalyst in the synthesis of pyrrole derivatives *via* the reaction of 2,5-hexanedione (**2**) and amines (**3**) (Scheme 2).



**Scheme 2.** Fe<sub>3</sub>O<sub>4</sub>@TiO<sub>2</sub>@(CH<sub>2</sub>)<sub>3</sub>OCO<sub>2</sub>Na-catalyzed synthesis of pyrrole **4**.

Firstly, in order to optimize the reaction conditions, the reaction of 2,5-hexanedione and aniline was selected as a model reaction. The model reaction was performed using Fe<sub>3</sub>O<sub>4</sub>@TiO<sub>2</sub>@(CH<sub>2</sub>)<sub>3</sub>OCO<sub>2</sub>Na at various conditions. On the basis of the results obtained, we found that this reaction was efficiently performed in the presence of 0.003 g of nanocatalyst **1** at 80 °C under solvent-free conditions (Table 1). A series of the product with different substituents was prepared from different aromatic amines bearing electron-withdrawing and electron-donating groups (Table 2). The structures of the obtained products were deduced from their FT-IR spectra and they were compared with authentic samples [26-28]. The synthesis of various pyrrole

derivatives has also been performed using other catalysts. Table 3 compares the production efficiency of product **4a** in the presence of different catalysts. According to this table, the nanocatalyst synthesized by us (Fe<sub>3</sub>O<sub>4</sub>@TiO<sub>2</sub>@(CH<sub>2</sub>)<sub>3</sub>OCO<sub>2</sub>Na), gives better efficiency in the shortest time using small amounts of catalyst. According to the nature of the substrate, catalyst and condition of the experiment, a most reasonable mechanism was advanced (Scheme 3). Initially, intermediate **5** is formed *via* condensation of the 1,4-dicarbonyl compound with amine in the presence of the catalyst. The compound **5** can lead to pyrroles following a cyclization and subsequent dehydration-aromatization route.

**Table 1.** Evaluating reaction conditions on model reaction.

Entry	Catalyst 1/g	Solvent	Temp./°C	Yield <sup>a</sup> /%
1	0.001	None	25	5
2	0.001	None	60	30
3	0.001	CH <sub>3</sub> OH	Reflux	10
4	0.001	CHCl <sub>3</sub>	reflux	15
5	0.001	H <sub>2</sub> O	reflux	10
6	0.002	None	60	50
7	0.003	None	60	83
8	0.004	None	60	80
9	0.003	None	80	90
10	0.003	None	100	85
11	0.003	Toluene	reflux	75
12	0.003	CHCl <sub>3</sub>	reflux	77
13	0.003	CH <sub>3</sub> OH	Reflux	70
14	0.003	H <sub>2</sub> O	reflux	70

<sup>a</sup> Isolated yield.

**Table 2.** Synthesis of pyrroles **4** in the presence of Fe<sub>3</sub>O<sub>4</sub>@TiO<sub>2</sub>@(CH<sub>2</sub>)<sub>3</sub>OCO<sub>2</sub>Na.

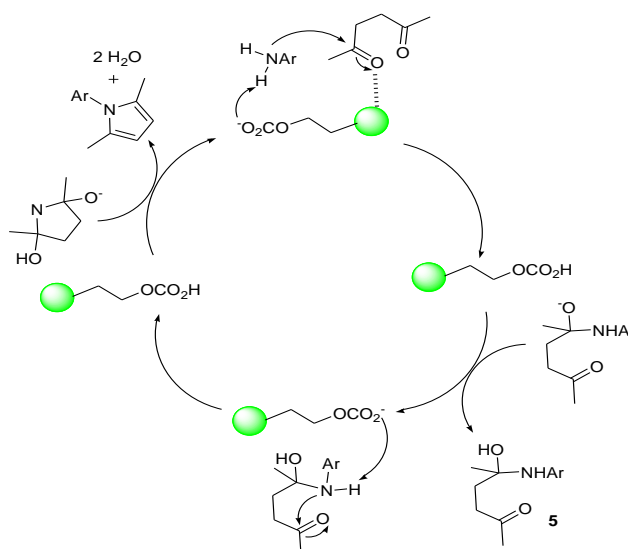
Entry	Ar	Time/min	M.p./°C	Yield <sup>a</sup> /%
4a	C <sub>6</sub> H <sub>5</sub>	20	49-51 [26]	96
4b	4-OCH <sub>3</sub> C <sub>6</sub> H <sub>4</sub>	15	58-60 [26]	81
4c	4-CH <sub>3</sub> C <sub>6</sub> H <sub>4</sub>	15	44-46 [27]	91
4d	4-NO <sub>2</sub> C <sub>6</sub> H <sub>4</sub>	20	142-144 [27]	90
4e	3-BrC <sub>6</sub> H <sub>4</sub>	25	73-75 [26]	87
4f	4-ClC <sub>6</sub> H <sub>4</sub>	25	75-77 [27]	92
4g	4-NH <sub>2</sub> C <sub>6</sub> H <sub>4</sub>	20	243-245 [26]	90
4h	2-CH <sub>3</sub> C <sub>6</sub> H <sub>4</sub>	20	57-60 [28]	80
4i	2-Naphthyl	20	118-120 [26]	83

<sup>a</sup> Isolated yield.

**Table 3.** Comparison of the efficiency of the Fe<sub>3</sub>O<sub>4</sub>@TiO<sub>2</sub>@(CH<sub>2</sub>)<sub>3</sub>OCO<sub>2</sub>Na nanocatalyst with other catalysts for the synthesis of **4a**.

Catalyst	Time (min)	Yield <sup>a</sup> (%)
Fe <sub>3</sub> O <sub>4</sub> @TiO <sub>2</sub> @(CH <sub>2</sub> ) <sub>3</sub> OCO <sub>2</sub> Na	20	96
UO <sub>2</sub> (NO <sub>3</sub> ) <sub>2</sub> .6H <sub>2</sub> O	30	94 [26]
BiCl <sub>3</sub> /SiO <sub>2</sub>	60	92 [28]
Sc(OTf) <sub>3</sub>	25	93 [8]
Ionic liquid	180	96 [13]

<sup>a</sup> Isolated yield.



**Scheme 3.** Proposed mechanism for the synthesis of pyrroles by nanocatalyst **1**.

The main drawback of some reported methods for Paal-Knorr synthesis of pyrroles is that the catalysts cannot be recovered or reused. In this work, to examine the reusability of the prepared nanocatalyst, after completion of the model reaction, the reaction mixture was diluted with ethanol and the catalyst was magnetically removed from it. Afterwards, the isolated catalyst was washed by distilled water and methanol and dried. The separated catalyst was directly used for the next run under the same conditions. The results showed that the catalyst can be reused without deactivation even after five cycles (Fig. 6).

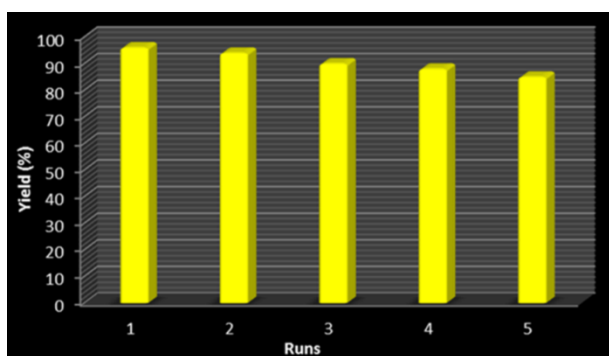


**Fig. 6.** Reusability study of nanocatalyst **1** in the synthesis of **4a** at 80 °C under solvent-free conditions.

## CONCLUSIONS

In summary, we introduced for the first time the preparation, characterization, and application of sodium carbonate immobilized on TiO<sub>2</sub>-coated Fe<sub>3</sub>O<sub>4</sub> nanoparticles (**1**). Fe<sub>3</sub>O<sub>4</sub>@TiO<sub>2</sub>@(CH<sub>2</sub>)<sub>3</sub>OCO<sub>2</sub>Na was characterized using FT-IR, XRD, SEM, EDS and VSM analysis. Some pyrrole derivatives as useful heterocycles were synthesized via the Paal-Knorr reaction using this catalyst. It can be stored for long times without significant loss in activity. The catalyst recyclability, mild conditions, high yield, short reacting times and long storage, are the main promising points of this work.

**Acknowledgement:** We gratefully acknowledge the partial support of this work by Yasouj University, Iran.

## REFERENCES

- M. A. Zolfigol, A. R. Moosavi-Zare, P. Moosavi, V. Khakyzadeh, A. Zare, *C. R. Chimie*, **16**, 962 (2013).
- A. Amoozadeh, S. Golian, S. Rahmani, *RSC Adv.*, **5**, 45974 (2015).
- M. Tajbakhsh, M. Farhang, R. Hosseinzadeh, Y. Sarrafi, *RSC Adv.*, **4**, 23116 (2014).
- R. B. Nasir Baig, R. S. Varma, *Chem. Commun.*, **49**, 752 (2013).
- W. Zhang, Y. Li, C. Wang, P. Wang, *Desalination*, **266**, 40 (2011).
- K. Koci, V. Matejka, P. Kovar, Z. Lacny, L. Obalova, *Catal. Today*, **161**, 105 (2011).
- K. Shimura, T. Miyazawa, T. Hanaoka, S. Hirata, *Appl. Catal. A*, **8**, 460 (2013).
- J. Chen, H. Wu, Z. Zheng, C. Jin, X. Zhang, W. Su, *Tetrahedron Lett.*, **47**, 5383 (2006).
- Y. H. He, G. Q. Wang, Z. Guan, *J. Heterocycl. Chem.*, **47**, 486 (2010).
- V. Amarnath, D. C. Anthony, K. Amarnath, W. M. Valentine, L. A. Wetterau, D. G. Graham, *J. Org. Chem.*, **56**, 6924 (1991).
- R. U. Braun, K. Zeitler, T. J. Muller, *J. Org. Lett.*, **3**, 3297 (2001).
- K. H. Lui, M. P. Sammes, *J. Chem. Soc. Perkin Trans.*, **1**, 457 (1990).
- B. Wang, Y. Gu, C. Luo, T. Yang, L. Yang, J. Suo, *Tetrahedron Lett.*, **45**, 3417 (2004).
- M. Farahi, B. Karami, R. Keshavarz, F. Khosravian, *RSC Adv.*, **7**, 46644 (2017).
- H. Mohamadi Tanuraghaj, M. Farahi, *RSC Adv.*, **8**, 27818 (2018).
- H. Mohamadi Tanuraghaj, M. Farahi, *New J. Chem.*, **43**, 4823 (2018).
- M. Farahi, F. Tamaddon, B. Karami, S. Pasdar, *Tetrahedron Lett.*, **56**, 1887 (2015).
- J. Etemad Gholtash, M. Farahi, *RSC Adv.*, **8**, 40962 (2018).
- F. Khosravian, B. Karami, M. Farahi, *New J. Chem.*, **41**, 11584 (2017).
- M. Farahi, B. Karami, Z. Rajabi Behesht Abad, S. Akrami, *Lett. Org. Chem.*, **14**, 612 (2017).
- F. Nemati, M. Heravi, D. Elhampour, *RSC Adv.*, **5**, 45775 (2015).
- M. A. Zolfigol, R. Ayazi-Nasrabadi, *RSC Adv.*, **6**, 69595 (2016).
- Z. Rashid, H. Naeimi, A. H. Zarnani, M. Nazari, M. Nejadmoghaddam, R. Ghahremanzadeh, *RSC Adv.*, **6**, 36840 (2016).
- K. Eskandari, B. Karami, S. Khodabakhshi, *Catal. Commun.*, **54**, 124 (2014).
- R. Chalasani, S. Vasudevan, *ACS Nano*, **7**, 4093 (2013).
- V. S. V. Satyanarayana, A. Sivakumar, *Ultrason. Sonochem.*, **18**, 917 (2011).
- O. Marvi, H. T. Nahzomi, *Bull. Chem. Soc. Ethiop.*, **32**, 139 (2018).
- K. Aghapoor, L. Ebadi-Nia, F. Mohsenzadeh, M. Mohebi Morad, Y. Balavar, H. R. Darabi, *J. Organomet. Chem.*, **708**, 25 (2012).